Transactions, SMiRT-26
Berlin/Potsdam, Germany, July 10-15, 2022
Special Session: Steam generator tube integrity

CONSIDERATION OF STEAM GENERATOR TUBING INTEGRITY

Xaver Schuler[1], Steffen Riehm[2], Bernd Gruhne[3], Jan Köhler[4]

[1] Head of Dep. QA Mech. Comp. EnBW Kernkraft GmbH, Neckarwestheim (x.schuler@kk.enbw.com)

[2] Head of Dep. Mech. Systems, EnBW Kernkraft GmbH, Neckarwestheim

[3] Senior Engineer NDE, EnBW Kernkraft GmbH, Neckarwestheim

[4] Head of Chemical Surveillance, EnBW Kernkraft GmbH, Neckarwestheim

INTRODUCTION

The nuclear power plant Neckarwestheim unit II (Gemeinschaftskraftwerk Neckar, GKN II) is a four loop PWR plant of Siemens/KWU Konvoi design with Alloy 800 steam generator (SG) tubing (shot peened). Due to the phase-out in Germany, the remaining operation time for GKN II will end in December 2022. During the regular outage in 2017, for the first time shallow pit-like volumetric indications (VI) on the outer diameter (OD) of SG tubes on the cold leg side of SG10 were detected by eddy current testing (ECT). During the outage in 2018, for the first time linear circumferential indications (CI) were detected on the OD of SG tubes on the hot leg side of SG20 and 40.

Because of the safety-related importance of SG tubes with respect to the heat removal from the primary circuit and confinement of radioactive materials, the integrity of the SG tubing must be ensured before continuing operation. This requires the consideration of several aspects as there are the evaluation of the findings acc. to the recommendations of nuclear regulations and standards, identification of the degradation mechanism and the root cause (root cause analysis), detection probability and inspection strategy of eddy current testing, fitness for service assessment, establishing of measures to eliminate the root cause and to mitigate the degradation mechanism during further operation, repair options and the adaptation of operational monitoring. Within this paper, these aspects will be discussed on the background of the experiences in GKN II.

RESULTS OF NON-DESTRUCTIVE EXAMINATION

The scope of eddy current testing (ECT) and the number of SG tubes with CI and VI detected during the outages 2017 to 2021 are summarized in Table 1. Most of the CI findings were located in SG20 on the hot leg (HL) side at or near by the upper transition of the upper roll expansion in areas with crevice corrosion of the ferritic tube sheet (TS), Figure 1. In the outage 2019 and the following, in addition to the X-Probe, the MRPC-Probe was used in areas with possible crevice corrosion to get more detailed information about size and distribution of the findings. This results in an additional number of detectable indications. The review of the 2018 X-Probe data revealed that a large number of CI detected in 2019 already did exist in 2018. The largest indications are multiple CI (MCI) distributed on the circumference of the SG tubes with a maximum local flaw depth of about 90% of the wall thickness (WT), Figure 2. Figure 3 shows the flaw characteristic of the two largest indications detected in the 2018 outage.

Table 1: History of indications

Scope of Eddy Current Testing	**Results**	
	No. of tubes with CI[1)]	**No. of tubes with VI**[2)]
Outage 2017 (Reportable event GKN II 03/2017)		
SG10, SG30 20% entire length (Bobbin) 10% X-Probe up to 1st support grid (HL+CL) after detection of VI at SG10 CL: 100% X-Probe up to 1st support grid at SG10 CL	No CI	SG10 CL: 32 HL: 0 **Σ: 32 tubes**
Outage 2018 (Reportable event GKN II 04/2018)		
all 4 SG (HL + CL) 20% entire length (Bobbin) 100% X-Probe up to 1st support grid, MRPC applied on tubes with linear indications from X-Probe testing	SG20 CL: 0 HL: 99 SG40 CL: 0 HL: 2 **Σ: 101 tubes**	SG10 CL: 9 HL: 2 SG20 CL: 0 HL: 1 SG30 CL: 6 HL: 0 SG40 CL: 5 HL: 0 **Σ: 23 tubes**
Outage 2019		
all 4 SG (HL+CL) Optimized test strategy: 100% X-Probe up to 1st support grid and MRPC at positions with tube sheet corrosion in the vicinity of the upper transition of the upper roll expansion (± 50 mm) Review of 2018 X-Probe data (values in ())	SG10 CL: 0 HL: 8+(2) SG20 CL: 0 HL: 63+(84) SG30 CL: 0 HL: 2 SG40 CL: 0 HL: 28+(4) **Σ: 101 + (90) tubes**	SG10 CL: 8 HL: 0 SG20 CL: 0 HL: 34 SG30 CL: 3 HL: 1 SG40 CL: 1 HL: 5 **Σ: 52 tubes**
Outage 2020		
all 4 SG (HL+CL) Test strategy according to outage 2019	SG20 CL: 0 HL: 6 SG40 CL: 0 HL: 1 **Σ: 7 tubes**	SG10 CL: 7 HL: 1 SG20 CL: 1 HL: 2 SG30 CL: 0 HL: 2 SG40 CL: 1 HL: 4 **Σ: 18 tubes**
Outage 2021		
all 4 SG (HL+CL) Test strategy according to outage 2019 plus 20% entire length (Bobbin) at SG10 and SG30	SG10 CL: 5 HL: 0 SG20 CL: 0 HL: (1) [3)] SG30 CL: 11 HL: 0 **Σ: 17 tubes**	SG10 CL: 3 SG20 HL: (1) [3)] SG30 CL: 1 **Σ: 5 tubes**

1) CI: linear circumferential indication on the outer diameter of tube
2) VI: shallow-pit-like volumetric indications on the outer diameter of tube
3) already present in the previous outage (result of data review from previous inspection)

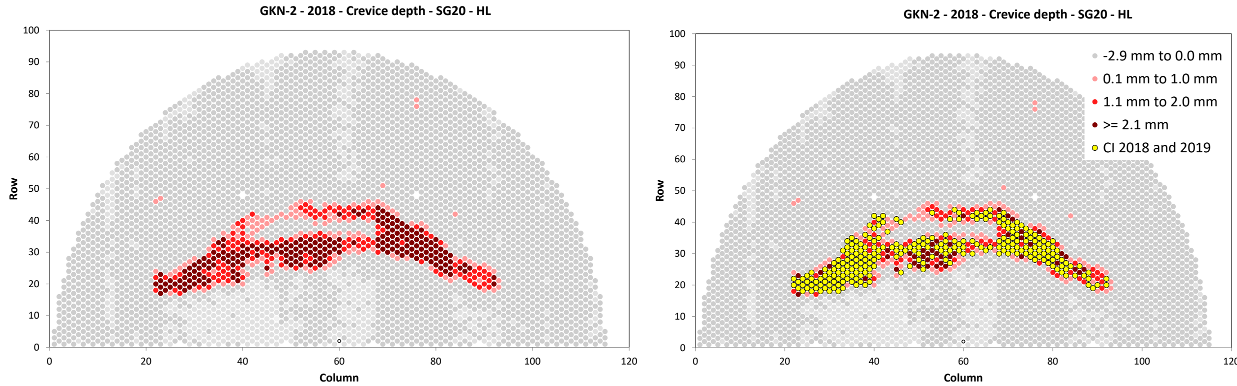

Figure 1: Location of CI in SG20 (right) related to crevice corrosion (crevice depth > 0) (left)

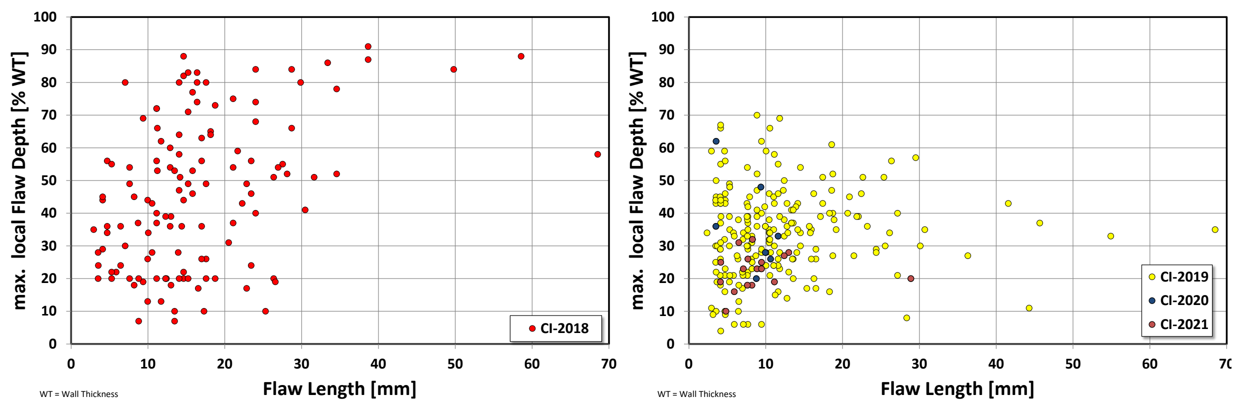

Figure 2: Size of CI detected in 2018 (left) and the following outages 2019, 2020 and 2021 (right)

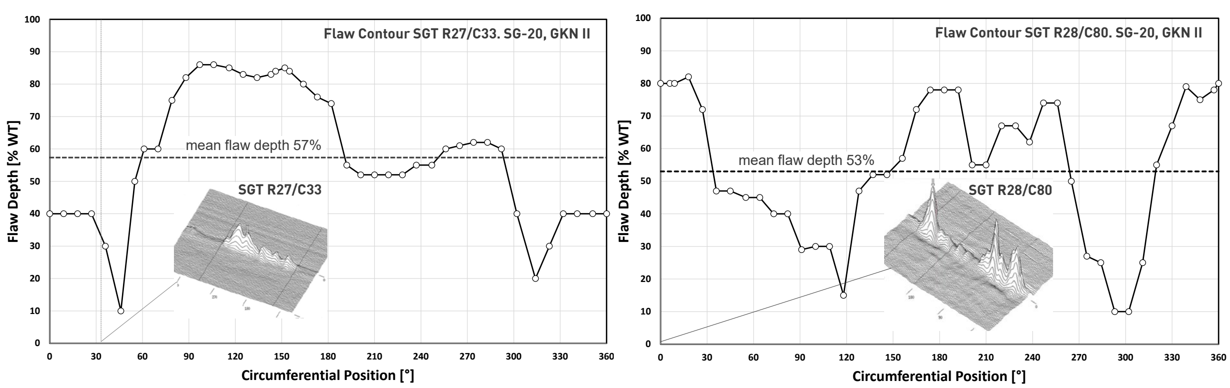

Figure 3: C-Scan and flaw contour determined by use of the amplitude signal of the MRPC-Probe

DEGRADATION MECHANISMS AND ROOT CAUSE ANALYSIS

The detailed root cause analysis performed in 2018 outage revealed the following degradation mechanisms. Outer Diameter Stress Corrosion Cracking (ODSCC) caused the crack-like circumferential linear indications (CI) at the upper transition of the upper roll expansion. The axial tensile stresses at this location are increased because of the crevice corrosion of the ferritic

TS and deepening of the crevices, Figure 4. Denting was detected at several SG tubes on the CL-side but at the HL-side, denting seems to be of minor importance. Pitting respectively inter granular attack (IGA) caused the pit-like volumetric indications (VI).

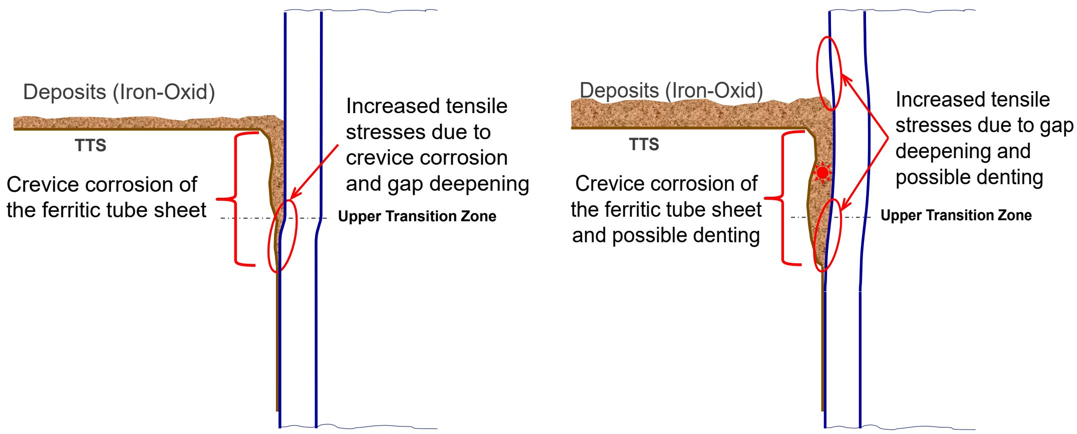

Figure 4: Zones of crevice corrosion and increased axial stresses without (left) and with denting (right)

The main root cause for these corrosion mechanisms was the increasing sulphate concentration in the feed water because of small, but persistent condenser leakages during the years 2013 to 2018, Figure 5. However, these leaks and the resulting ingress of sulphate in the feed water were still within the permissible limits of the VGB Standard (2006). Never the less, the enrichment of these sulphate impurities in the iron oxide deposits on the Top of the Tube Sheet (TTS) and SG tube surfaces caused the observed findings.

The cause of the condenser leakages was identified as droplet impact erosion. Hence, the leak detection was very difficult because of the very tiny leaks caused by this mechanism and the adverse conditions for leakage tests in the large four-flow exhaust section.

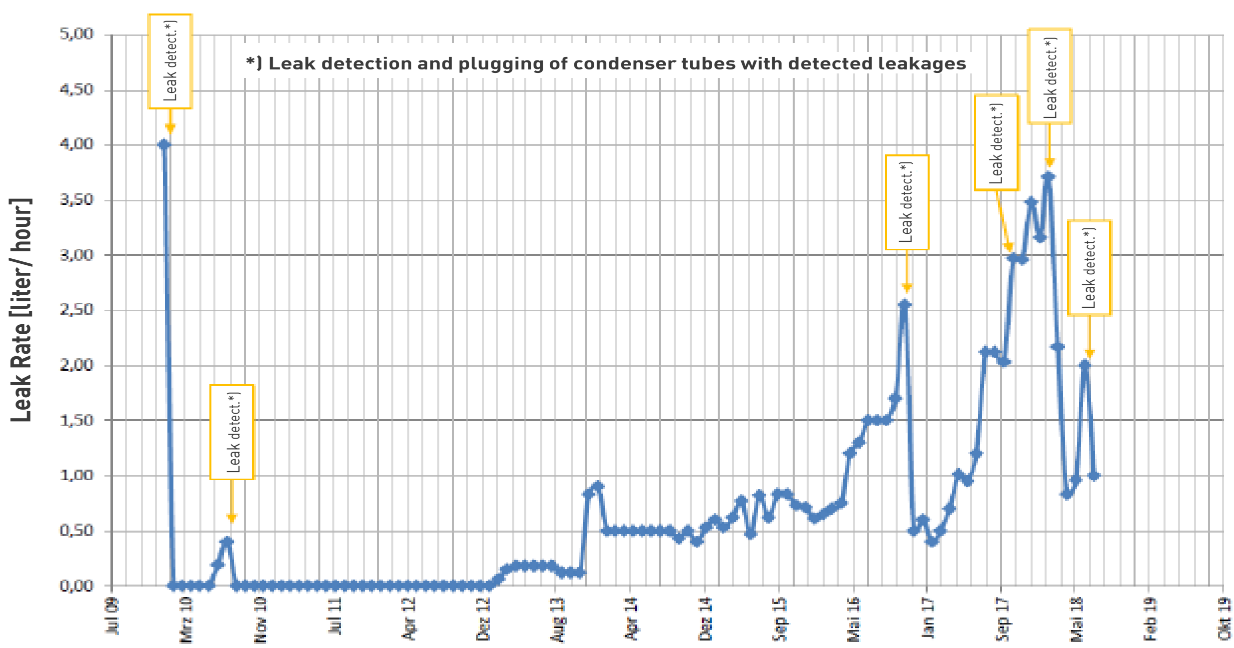

Figure 5: Persistent condenser leakages during the years 2013 to 2018

FITNESS FOR SERVICE ASSESSMENT

According to SiAnf (2015), Annex 2, the failure of a SG tube with a leakage rate above the operationally permissible rate up to the maximum SG tube leak of a double ended guillotine break has to be treated as a design basis accident. In ageing management in accordance with KTA 1403 (2017), the SG tubes have to be assigned to group M2, for which preventive maintenance has to be carried out. This is to prevent ageing-related failures due to common mode failure. According to RSK Recommendation (2019), degradation of SG tubes must be detected in good time by suitable non-destructive testing methods so that a failure of SG tubes need not be postulated until the next inspection. In this case, SG tube failure is defined as a leakage that is greater than the operationally permissible leakage. The assessment procedure to evaluate the results of in-service inspection (ISI) and to guarantee the integrity of SG tubes is based on KTA 3201.4 (2016).

The fitness for service assessment of SG tubes consists of the following two steps. The first step includes the integrity analysis of the findings to evaluate remaining safety margins for normal operation as well as postulated emergency and faulted conditions. The second step consists of the integrity analysis, including leak-before-break (LBB) assessment of the postulated flaw evolution during the subsequent operation period.

The calculation methods used are fracture mechanics approaches, as there are flow stress concept (FSK/MPA) and R6-Method acc. to KTA 3206 (2014), Appendix B, as well as elastic-plastic finite element (FE) analyses. The conservativism of theses calculation methods were verified by experimental investigations and numerical FE-analyses using local approach models, see BMU (2013) and Gehrlicher et al. (2013).

The relevant load cases and related loads are listed in Table 2. Regarding the stresses near the tube sheet, the covering load case in GKN II for postulated emergency and faulted conditions (Level C and D) is the ATWS load case. In addition to the differential pressure between primary and secondary side, the fluid dynamic loading of the SG tubes between TS and first support grid was considered by the application of a global bending moment of 9.1 Nm conservatively. For the relevant dimensions and boundary conditions, see Figure 6.

Table 2: Relevant load cases and loads for the steam generators of GKN II

Load Case	p_{prim}	p_{sec}	Δp_{max}	M_b 1)	Temperature			
					$T_{prim,HL}$	$T_{prim,CL}$	T_{sec}	$T_{m,HL}$ 2)
	[MPa]	[MPa]	[MPa]	[Nm]	[°C]	[°C]	[°C]	[°C]
Normal Operation	15.49	5.88	9.37	9.1	326	292	274	297
Upset Conditions	15.60	5.50	10.10	9.1	319	290	270	295
Emergency Condition (ATWS, Level C)	22.80	7.30	15.50	9.1	358	354	293	326

1) Bending moment due to fluid structure interaction (design specification)
2) Mean temperature of SG tubes at hot leg side

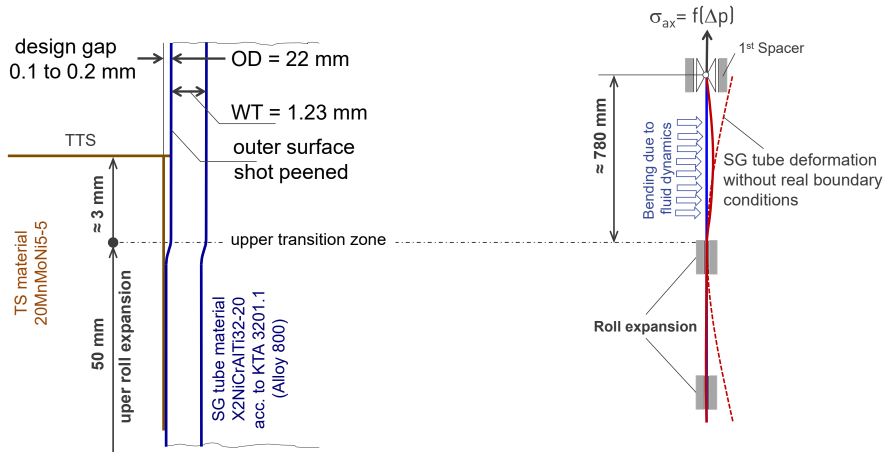

Figure 6: Relevant dimensions in the zone of findings (left) and boundary conditions (right)

In a first approach, the limit load of SG tubes with circumferential flaws of constant depth was determined based on simplified and conservative fracture mechanics (FM) calculations using the FSK/MPA- and R6-Method. For the covering ATWS load case, the maximum calculated critical flaw depth using the FSK/MPA method was 80% WT, Figure 7 (left). For this flaw depth the R6-Method calculated a maximum differential pressure of Δp=17.5 MPa, Figure 7 (right), that is above the value of 15.5 MPa for the ATWS load case. This shows a large safety margin compared to the mean flaw depth of 57% WT of the largest finding, see Figure 3 (left).

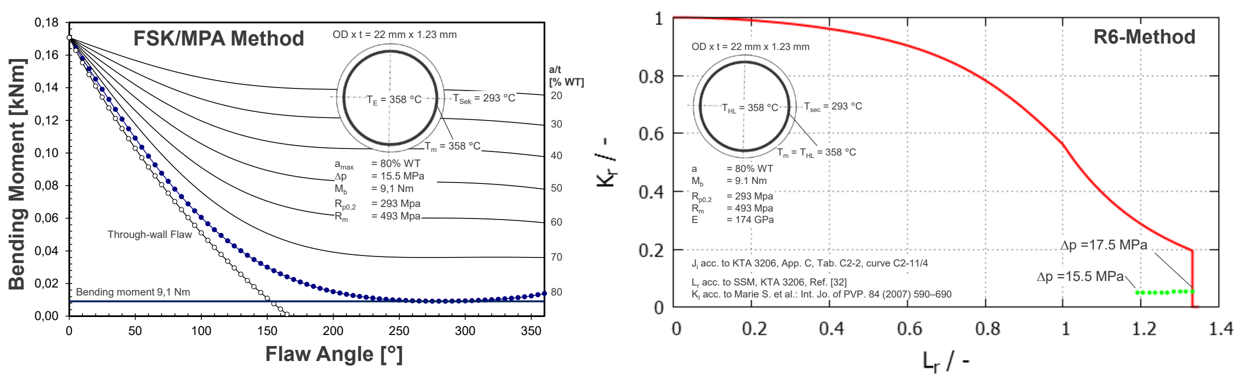

Figure 7: Result of fracture mechanics calculations with FSK/MPA- (left) and R6-Method (right)

In addition to these calculations, finite element (FE) analyses were performed, considering the real flaw contour and realistic boundary conditions, Figure 6 (right), as well as elastic-plastic material behavior based on lower bound stress-strain curves. For the largest finding, Figure 3 (left), the calculated failure pressure Δp (plastic limit load) was 44 MPa, Figure 8, which is a safety margin (SM) of SM=2.8 compared to the ATWS load case. The FE-analysis based on the mean value of the flaw depth of 57% WT shows nearly the identical load-bearing curve and failure pressure. These calculations also confirms the conservatism of the MPA/FSK calculation based on the mean value of the flaw depth (SM=2.6, see Figure 8).

To ensure the SG tube integrity during the subsequent operation period, the conservative estimation of flaw evolution was based on the evaluation of the worldwide operational experience on SG tubes with ODSCC findings and especially of Siemens/KWU SGs. Based on this evaluation a conservative estimation on the flaw evolution until the next inspection (= next outage) were made. The flaw growth was postulated up to 70% of WT constant over the full circumference. Additionally, within the framework of the LBB-assessment, a local through-wall flaw up to the critical flaw length was assumed. For this flaw configuration, the calculated critical through-wall flaw length was 10.5 mm (flaw angle $2\alpha_{LBB} = 55°$) by use of the FSK/MPA- and R6-method respectively, Figure 9 (left). In comparison with the FE analysis, taking into account the real boundary conditions of the SG tubes, the great conservatism of the simplified FM calculations becomes apparent. For the maximum emergency and faulted conditions (ATWS load case), flaw angles up to $2\alpha = 120°$ are still stable, Figure 9 (right).

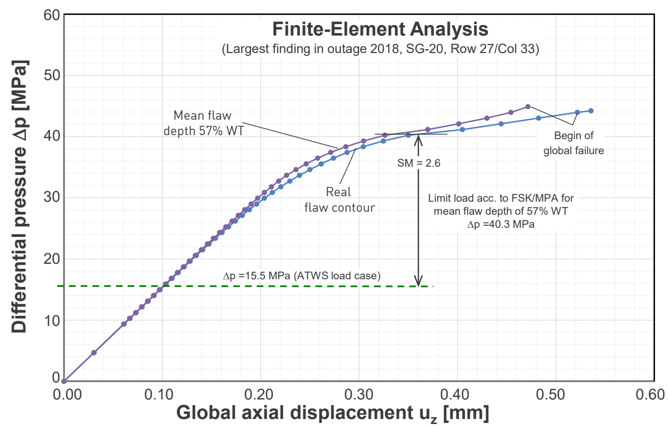

Figure 8: Load bearing behavior determined by elastic-plastic FE-analyses

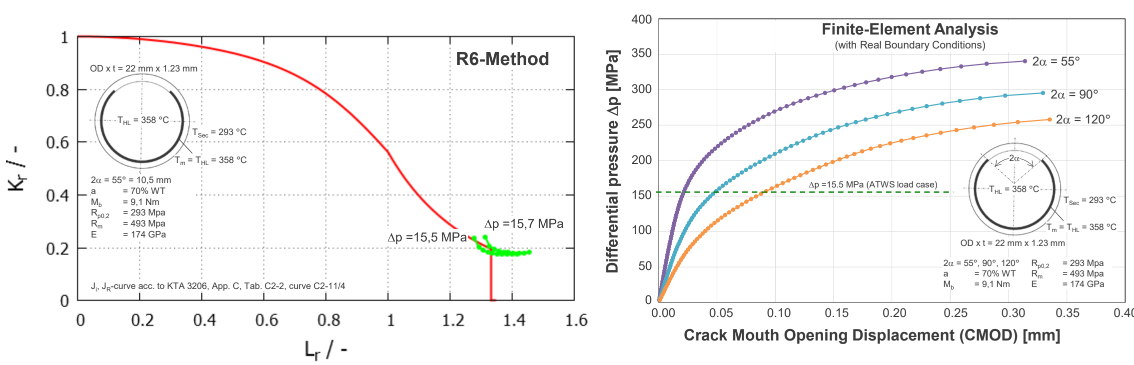

Figure 9: LBB-Assessment: Calculation of critical through-wall flaws length

For the LBB-assessment, the calculation of the leak rate as a function of flaw length for normal operating conditions is necessary. This calculation was performed using the leak rate models “modified Bernoulli” and “homogenous equilibrium model (HEM)” acc. to KTA 3206 (2014), App. B 3.2.2.2 and B 3.2.2.3 respectively. The leak opening area was calculated using linear-elastic material behaviour and the postulated circumferential flaw depth of 70% WT was not taken into account. This is conservative related to leak rate detectability. Figure 10 shows the results of these calculations in comparison with the detectability limit (0.02 kg/h) and shut down criteria (0.04 kg/h). Even for the shortest calculated critical through-wall flaw size of $2\alpha_{LBB} = 55°$, see Figure 9 (left), the safety margin with respect to LBB is greater than a safety margin of

SM_{Leak}=10. This LBB-assessment demonstrates large safety margins with respect to the SG tube integrity for the subsequent operation period.

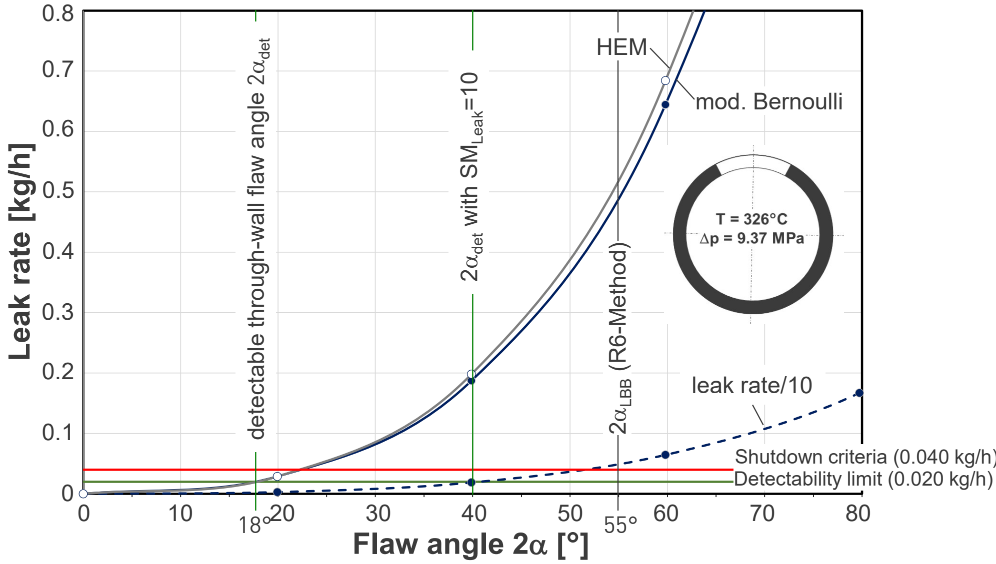

Figure 10: LBB-Assessment

REMEDIAL MAINTENANCE AND MITIGATIVE MEASURES

All linear indication (independent of flaw size) were stabilized using filler plugs and sealed with rolled plugs, acc. to the recommendations of the reactor safety commission, see RSK Recommendation (2019). Volumetric indications with ≥ 30% wall thinning were preventive plugged with rolled plugs.

The most important remedial measure was to prevent further condenser leakages. After identifying the degradation mechanism "droplet impact erosion", it was possible to identify the most affected condenser tubes for preventive plugging, Figure 11 (left). After preventive plugging of more than 2,000 condenser tubes, no further condenser leakages occurred.

The second important measure was the mechanical TTS cleaning in the outage of 2018 to remove the soft sludge with most of the sulphate inventory of the SGs, Figure 11 (right).

In order to neutralize the conditions in the crevices and deposits as far as possible, extensive flushing programs with accompanying chemical analyses were performed and continued during all subsequent outages.

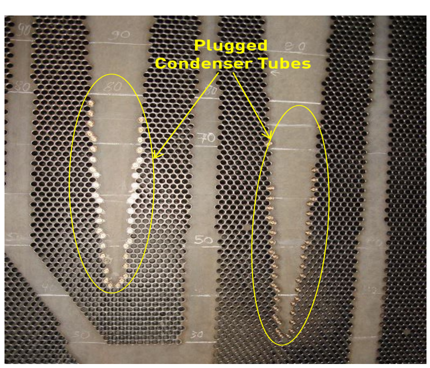

Figure 11: Preventive plugging of condenser tubes (left), mechanical SG TTS-cleaning (right)

The statistical evaluation of the findings confirms the efficiency of the implemented measures, Figure 12.

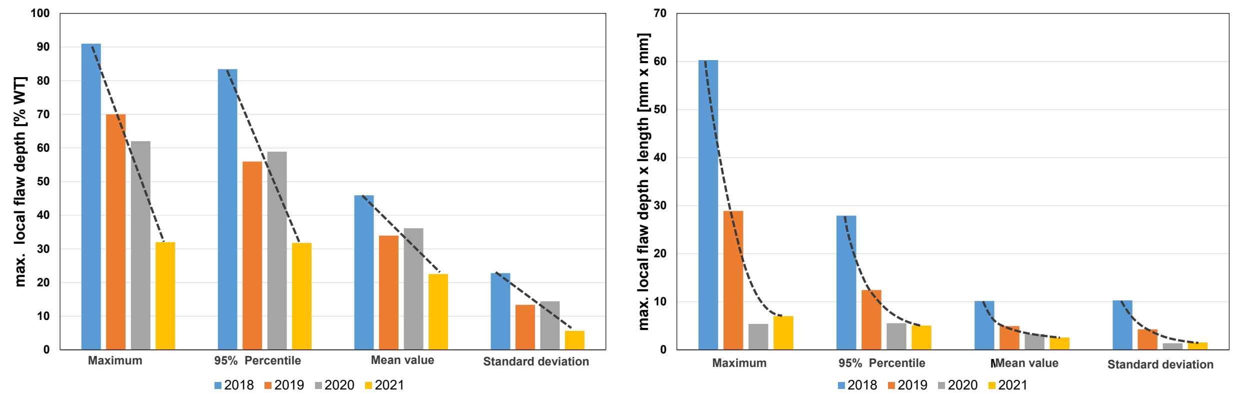

Figure 12: Statistical evaluation of maximum local flaw depth (left) and flaw size (right)

OPERATIONAL SURVEILLANCE

As a consequence of the GKN II SG experience, the VGB guideline for the water chemistry of LWR Plants was revised. The most important modification was the implementation of integral control parameters for the surveillance of longer ingress periods of even small amounts of ionic impurities, see e.g. for sulphate ingress Figure 13 (left). Since the preventive plugging of condenser tubes and the cleaning and flushing measures, all control parameter of the secondary water chemistry are within and mostly below the normal operating range, see e.g. sulphate concentration Figure 13 (right).

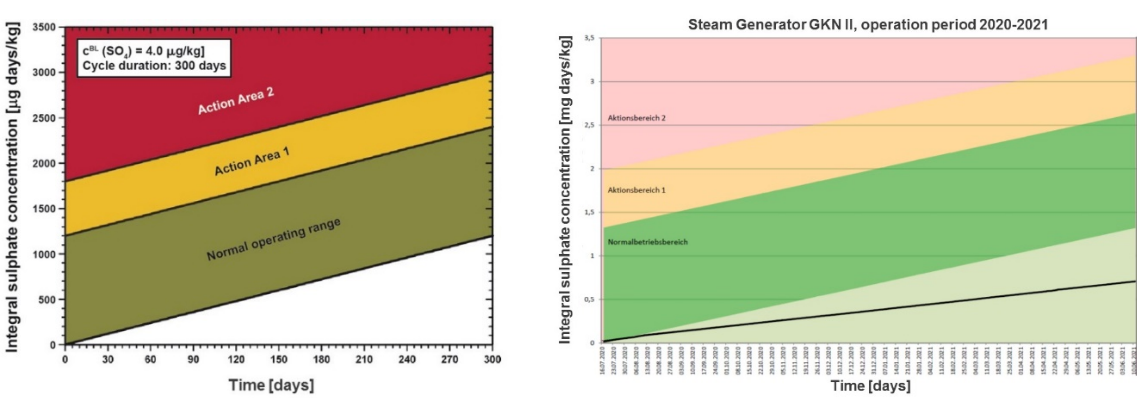

Figure 13: Integral control parameter for sulphate ingress acc. to VGB Standard (2020) (left) and GKN II SG data for the operation period 2020-2021 (right)

The RSK recommendation (2019) recommends, “The operating rules have to contain provisions to ensure that SG tube leakages are detected with certainty before any cracks reach a critical length and that in this case, the plant is shut down immediately”. The continuous SG tube leak detection in GKN II is based on the high sensitivity of the activity control sensors in the blowdown lines. This activity control is able to detect very small SG tube leakages with leak rates of ≥ 0.02 kg/h. The shutdown criteria of 0.04 kg/h, as defined in the operating rules of GKN II, fulfils the RSK recommendation and includes a large safety margin with respect to LBB, see Figure 10.

CONCLUSIONS

The root cause of the degradation mechanism was ODSCC and pitting corrosion respectively IGA as a result of condenser leakages caused by droplet impact erosion and the enrichment of sulfate in the SG iron oxide deposits on the top of the tube sheet and SG tube surfaces. Most of the indications were located in areas with tube sheet corrosion. All linear indication (independent of flaw size) were stabilized using filler plugs and sealed with rolled plugs. Volumetric indications with ≥ 30% wall thinning were preventively plugged with rolled plugs. Due to the high sensitivity of the activity control sensors in the blow down lines, very small SG tube leakages are detectable. The fitness for service assessment confirmed the high load bearing capacity of the flawed SG tubes and large safety margins with respect to Leak-Before-Break. To eliminate the root cause for the ingress of sulphate a large number of more than 2,000 of the 63,000 condenser tubes were plugged preventively. The mechanical tube sheet cleaning performed in the 2018 outage and flushing programs continued during the subsequent outages remove most of the sulphate inventory and neutralize the conditions in the crevices and deposits continuously. During the last outages in 2020 and 2021, only a few new and small indications were detected. This confirms the efficiency of the implemented measures to ensure a safe and reliable operation until end of 2022 and the conservatism of the fitness for service assessment.

REFERENCES

BMU (2013) Forschungsvorhaben 3610R01385. „Schädigungsmechanische Modellierung des Resttragvermögens von geschädigten Dampferzeugerheizrohren“, *BMU*, Abschlussbericht, Juli 2013.

Gehrlicher, S., X. Schuler, M. Seidenfuss, J. Mahlke (2013). „Damage Modeling of the Load-Bearing Capacity of Damaged Steam Generator Tubes in Nuclear Power Plants”, *Proceedings of ASME PVP-Conference*, ASME Pressure Vessels & Piping Conference, July 14–18, 2013, Paris, France.

KTA 3201.4 (2016). “Components of the Reactor Coolant Pressure Boundary of Light Water Reactors, Part 4: In-service Inspections and Operational Monitoring”, *Safety Standards of the Nuclear Safety Standards Commission (KTA),* November 2016.

KTA 1403 (2017). “Ageing-Management in Nuclear Power Plants”, *Safety Standards of the Nuclear Safety Standards Commission (KTA),* November 2017.

KTA 3206 (2014). “Break Preclusion Verifications for Pressure-Retaining Components in Nuclear Power Plants”, *Safety Standards of the Nuclear Safety Standards Commission (KTA)*, November 2014.

RSK Recommendation (2019). “Damage on steam generator (SG) tubes caused by stress corrosion cracking – Measures to ensure the integrity of the tubes”, 512th meeting of the Reactor Safety Commission (RSK), October 22-23, 2019.

SiAnf (2015). “Safety Requirements for Nuclear Power Plants - Rules and Regulations for Nuclear Safety and Radiation Protection” *Bundesamt für Strahlenschutz*, Edition March 2015.

VGB-Standard (2006). VGB-R 401 J, VGB-Standard for the Water in Nuclear Power Plants with Light-Water Reactors, *VGB PowerTech*, 2006.

VGB Standard (2020)., VGB-Standard for the Water in Nuclear Power Plants with Light-Water Reactors (Formerly VGB-R 401 J), *VGB PowerTech*, May 2020.